A PROJECTION METHOD WITH REGULARIZATION FOR THE CAUCHY PROBLEM OF THE HELMHOLTZ EQUATION*

Yunyun Ma,   Fuming Ma   and   Heping Dong

School of Mathematics, Jilin University, Changchun 130012, China
Email: mayy2009@gmail.com, mafm@jlu.edu.cn, dhp@jlu.edu.cn

Abstract

This paper is concerned with the reconstruction of the radiation wave field in the exterior of a bounded two- or three-dimensional domain from the knowledge of Cauchy data on a part of the boundary of the aforementioned domain. It is described by the Cauchy problem for the Helmholtz equation. By using the Dirichlet-to-Neumann map, this problem is transformed into an operator equation with compact operator. We rigorously justify the asymptotic behaviors of singular values of the compact operator. Then a projection method with regularization is applied to solve the operator equation, and the convergence of the regularization method is discussed. Finally, several numerical examples are presented to illustrate the approach. The results demonstrate that the algorithm is effective.

Mathematics subject classification: 35R25, 35R30, 78A40.
Key words: Helmholtz equation, Cauchy Problem, Projection method, Regularization.

1. Introduction

The Helmholtz equation arises naturally in many physical applications related to wave propagation and vibration phenomena (see, e.g., [3, 6, 7, 19] and the references therein). It is often used to describe the vibration of a structure, the radiation wave and the scattering of a wave. We focus on the determination of the radiation wave field in this study.

The theoretical and numerical studies on the Helmholtz equation have been developed extensively in the past century. Most of the results studying on the numerical methods of the Helmholtz equation are related with the boundary value problems, i.e., the Dirichlet, Neumann or mixed boundary value problems (see, e.g., [1, 4, 10, 12, 14]). The well-posedness of the boundary value problems of the Helmholtz equation via the removal of the eigenvalues of the Laplacian operator is well established. Unfortunately, many engineering problems do not belong to this category. In particular, the boundary conditions are often incomplete, either in the form of the underspecified and overspecified boundary conditions on the different parts of the boundary or the solution is prescribed at some internal points in the domain. These problems are usually ill-posed, i.e., the existence, uniqueness and stability of their solutions are not always guaranteed.

Motivated by the advance in the measurement technology, the wave field and its gradient can be collected at a portion of a closed surface. Therefore, many important studies have been devoted to the Cauchy problem associated with the Helmholtz equation, which is severely ill-posed [13]. The determination of the sources was discussed in [9]. The reconstruction of the radiation field was discussed in [26]. Unlike the boundary value problems, the uniqueness of

the Cauchy problem is guaranteed without the necessity of removing the eigenvalues for the Laplacian. However, the Cauchy problem suffers from the non-existence and instability of the solution. A number of numerical methods have been proposed to solve this problem, such as the iterative algorithm proposed by Kozlov et al. [17,18,21,22], the spherical wave expansion method [30,31], the Fourier regularization method [8,27], the method of fundamental solution [23], the boundary knot method [15], the plane wave method [16], the boundary element-minimal error method [24], and the moment method [28,29].

In this paper, we propose a numerical method dealing with the Cauchy problem for the Helmholtz equation in the exterior of a bounded two- or three-dimensional domain. The paper is organized as follows. In Section 2, we formulate the problem and transform the Cauchy problem into an operator equation with a compact operator. In Section 3, we discuss the regularity properties of the compact operator and propose a projection method with regularization for solving the compact operator equation in the two-dimensional case. Section 4 provides the projection method with regularization for the reconstruction of the radiation wave field in the three-dimensional case, which is a little different from the two-dimensional case. In Section 5, we show several numerical examples to demonstrate the effectiveness of our method. Finally, a short conclusion in Section 6 summarizes the results of this paper.

2. Mathematical Formulation of the Problem

Consider the reconstruction of the radiation wave field arising from the sources of radiation. Let B_R be a ball of radius R centered at the origin in $\mathbb{R}^d$ ($d = 2, 3$). It contains all the sources of the wave field. When a time harmonic wave is considered, the propagation of the waves in the homogeneous isotropic medium is governed by the Helmholtz equation

$$\triangle u + k^2 u = 0 \ \ \text{in } \mathbb{R}^d \setminus \overline{B_R}, \tag{2.1}$$

with the Sommerfeld radiation condition

$$\lim_{r \to \infty} r^{\frac{d-1}{2}} \left(\frac{\partial u}{\partial r} - \mathrm{i}ku \right) = 0, \quad r = |x|, \tag{2.2}$$

where $k = w/c > 0$ is the wave number with the angular frequency w and the speed of sound c. $\mathrm{i} = \sqrt{-1}$ is the imaginary unit.

In this paper, both the wave field f and its normal derivative g on Γ, where $\Gamma \subset \partial B_R$ is an open set, are considered as the input data for the reconstruction of the radiation wave field in the domain $\mathbb{R}^d \setminus B_R$. Hence, the problem can be formulated as finding a radiation solution $u \in C^2(\mathbb{R}^d \setminus \overline{B_R}) \cap C(\mathbb{R}^d \setminus B_R)$ of the equation (2.1)–(2.2), which satisfies the Cauchy condition

$$u = f, \ \ \frac{\partial u}{\partial n} = g, \ \ \text{on } \Gamma, \tag{2.3}$$

where $\vec{n}$ is the unit outward normal of the boundary Γ.

Suppose the Cauchy problem (2.1)–(2.3) has a solution $u \in C^2(\mathbb{R}^d \setminus \overline{B_R}) \cap C(\mathbb{R}^d \setminus B_R)$. Denote $u = \tilde{f}$ on ∂B_R. It is well known that if $\tilde{f}$ on ∂B_R is given, the radiation solution u of the Helmholtz equation (2.1) satisfying the radiation condition (2.2) is unique determined (see, e.g., [2, Chapter 3]). Let Λ be the Dirichlet-to-Neumann map, which is defined by

$$\Lambda \tilde{f} = \frac{\partial u}{\partial n} \Big|_{\partial B_R}.$$

Given $s \geq 0$, by $H^s(\partial B_R)$ we denote the Sobolev space on ∂B_R (see, e.g., [20, Chapter 3]). We define the operator $K : H^d(\partial B_R) \to [L^2(\Gamma)]^2$ by

$$K\tilde{f} = \left(\tilde{f}\Big|_\Gamma, \Lambda\tilde{f}\Big|_\Gamma \right), \quad \text{for } \tilde{f} \in H^d(\partial B_R).$$

Then the Cauchy problem (2.1)–(2.3) is transformed into the compact operator equation as follows.

Problem 1. *Given $f, g \in L^2(\Gamma)$, find a function $\tilde{f} \in H^d(\partial B_R)$ satisfying*

$$K\tilde{f} = (f, g). \tag{2.4}$$

In the following sections, we will briefly discuss the regularity properties of K and show the projection method with regularization for solving (2.4).

3. The Two-Dimensional Case

Set $w(t) = \left(R\cos t, R\sin t \right)$, where $t \in [0, 2\pi]$. Then $\psi \in H^s(\partial B_R)$ $(s > 0)$ if and only if $\psi \circ w \in H^s[0, 2\pi]$. By $\psi \circ w$, as usual, we mean the function given by $(\psi \circ w)(t) = \psi(w(t))$, $t \in [0, 2\pi]$. Meanwhile the inner product and norm in $H^s(\partial B_R)$ are defined by

$$\langle \varphi, \psi \rangle_s := \sum_{n \in \mathbb{Z}} 2\pi \left(1 + n^2\right)^s a_n \overline{b}_n$$

and $\| \cdot \|_s = \langle \cdot, \cdot \rangle_s^{1/2}$, where a_n and b_n are the Fourier coefficients of $\varphi \circ w$ and $\psi \circ w$ (see, e.g., [19]). For $F = (f_1, f_2)$, $G = (g_1, g_2) \in [L^2(\Gamma)]^2$, the inner product in $[L^2(\Gamma)]^2$ is given by

$$\langle F, G \rangle = \int_\Gamma \left(f_1\overline{g_1} + f_2\overline{g_2} \right) \mathrm{d}s.$$

In the two-dimensional case, a radiation solution to the Helmholtz equation in the exterior of B_R has an expansion (see, e.g., [3, Chapter 2])

$$u(r, t) = \sum_{n \in \mathbb{Z}} \frac{c_n}{H_{|n|}(kR)} H_{|n|}(kr)\mathrm{e}^{int}, \quad t \in [0, 2\pi], \tag{3.1}$$

where $H_{|n|}$ are the Hankel functions of the first kind of order $|n|$ and c_n are the Fourier coefficients of $u(R, t)$. From [5, Lemma 2.1], we have $H_n(kR) \neq 0$ for any $n \in \mathbb{Z}$, $R > 0$. It is therefore reasonable that $H_n(kR)$ are in the denominator. In particular, the normal derivative $\Lambda\tilde{f}$ has the form

$$\Lambda\tilde{f} = \sum_{n \in \mathbb{Z}} c_n Z_n(kR)\mathrm{e}^{int},$$

where

$$Z_n(kR) = \frac{n}{R} - \frac{kH_{|n|+1}(kR)}{H_{|n|}(kR)}. \tag{3.2}$$

Then the problem is formulated as follows.

Problem 2. *Given f, $g \in L^2(\Gamma)$, find a function $\tilde{f} = \sum_{n \in \mathbb{Z}} c_n\mathrm{e}^{int} \in H^2(\partial B_R)$ satisfying*

$$\tilde{f} = f, \quad \Lambda\tilde{f} = g, \quad \text{on } \Gamma. \tag{3.3}$$

3.1. Ill-posedness of the problem

Recalling the definition of the operator K in the formulation of the Cauchy problem of the Helmholtz equation mentioned above and the compactness of the imbedding operators from $H^2(\Gamma)$ and $H^1(\Gamma)$ to $L^2(\Gamma)$ (see, e.g., [20, Chapter 3]), we obtain that

Theorem 3.1. $K : H^2(\partial B_R) \to \left[L^2(\Gamma) \right]^2$ *is a compact operator.*

Therefore, the Cauchy problem of the Helmholtz equation considered here is ill-posed. Furthermore, it is expected that the measure of Γ has impact on the ill-posedness of the problem, which is illustrated by the rate of the convergence of singular values of the operator K. Unfortunately, we can not explicitly determine the singular values of K. But we can state the following behaviors.

Theorem 3.2. *Let* $\mathrm{meas}(\Gamma)$ *stand for the measure of* Γ. *For the eigenvalues* $\mu_n(K^*K)$ *of* K^*K, *we have the estimation*

$$\mu_n(K^*K) \lesssim \frac{1}{n^{\frac{\rho}{2}}}\mathrm{meas}(\Gamma), \quad n \to \infty, \tag{3.4}$$

where $0 < \rho < 1$ *and* K^* *denotes the adjoint operator of* K. $A \lesssim B$ *means* $A \leqslant cB$ *with a constant* $c > 0$.

Proof. Given $\tilde{f} = \sum\limits_{n\in\mathbb{Z}} c_n \mathrm{e}^{int} \in H^2(\partial B_R)$ and $\tilde{h} = \sum\limits_{n\in\mathbb{Z}} d_n \mathrm{e}^{int} \in H^2(\partial B_R)$, we have that

$$\langle K\tilde{f}, K\tilde{h} \rangle = \sum_{n\in\mathbb{Z}} \sum_{m\in\mathbb{Z}} c_m \overline{d_n} \langle \mathrm{e}^{imt}, \mathrm{e}^{int} \rangle_{L^2(\Gamma)}$$
$$+ \sum_{n\in\mathbb{Z}} \sum_{m\in\mathbb{Z}} c_m Z_m(kR) \overline{d_n Z_n(kR)} \langle \mathrm{e}^{imt}, \mathrm{e}^{int} \rangle_{L^2(\Gamma)}$$
$$= \sum_{n\in\mathbb{Z}} \overline{d_n} \Big(\sum_{m\in\mathbb{Z}} \Big(1 + Z_m(kR) \overline{Z_n(kR)} \Big) c_m \langle \mathrm{e}^{imt}, \mathrm{e}^{int} \rangle_{L^2(\Gamma)} \Big). \tag{3.5}$$

Let $A_{nm} = \langle \mathrm{e}^{imt}, \mathrm{e}^{int} \rangle_{L^2(\Gamma)}$ and

$$\hat{f} = \sum_{n\in\mathbb{Z}} \frac{1}{2\pi(1+n^2)^2} \Big(\sum_{m\in\mathbb{Z}} \Big(1 + Z_m(kR) \overline{Z_n(kR)} \Big) c_m A_{mn} \Big) \mathrm{e}^{int}. \tag{3.6}$$

It is easy to check that $|A_{nm}| < \mathrm{meas}(\Gamma)$. According to the above deduction and the relation

$$\langle \hat{f}, \tilde{h} \rangle_2 = \langle K\tilde{f}, K\tilde{h} \rangle = \langle K^*K\tilde{f}, \tilde{h} \rangle_2$$

for all $\tilde{h} \in H^2(\partial B_R)$, we obtain that the operator $K^*K : H^2(\partial B_R) \to H^2(\partial B_R)$ is given by

$$\hat{f} = K^*K\tilde{f}.$$

Introducing

$$A_N \tilde{f} = \sum_{|n|\leq N} \frac{1}{2\pi(1+n^2)^2} \Big(\sum_{m\in\mathbb{Z}} \Big(1 + Z_m(kR) \overline{Z_n(kR)} \Big) c_m A_{mn} \Big) \mathrm{e}^{int}, \tag{3.7}$$

we observe that

$$A_N(H^2(\partial B_R)) \subset \mathrm{span}\Big\{ \mathrm{e}^{int}, 0 \leqslant |n| \leqslant N \Big\}$$

and $\dim A_N(H^2(\partial B_R)) \leqslant 2N + 1$. It means that A_N has at most $2N + 1$ non-vanishing eigenvalues. The min-max principle on the self-adjoint operator, which can be found in [25, Chapter 13], gives the relation

$$\begin{aligned}
\mu_{2N+2}(K^*K) &\leq \mu_{2N+2}(A_N) + \mu_1(K^*K - A_N) \\
&\leq 0 + \|K^*K - A_N\|_2,
\end{aligned} \tag{3.8}$$

where $\mu_n(A)$ denote the nth eigenvalue of the self-adjoint operator A with $\mu_n(A) \geq \mu_{n+1}(A)$, $n \in \mathbb{N}$.

Next, we estimate $\|K^*K - A_N\|_2$. From the asymptotic behaviors of

$$H_n(t) = \frac{2^n(n-1)!}{\pi \mathrm{i} t}(1 + O(\frac{1}{n})), \quad n \to \infty$$

(see, e.g., [3, Chapter 2]), it is obvious that

$$Z_n(kR) = -\frac{2n}{R}(1 + O(\frac{1}{n})), \quad n \to \infty. \tag{3.9}$$

From the Cauchy inequality, we obtain that

$$\begin{aligned}
&\|(K^*K - A_N)\tilde{f}\|_2^2 \\
&= \sum_{|n| \leq N} \frac{1}{2\pi(1+n^2)^2}\Big|\sum_{|m|>N}(1 + Z_m(kR)\overline{Z_n(kR)})c_m A_{mn}\Big|^2 \\
&\quad + \sum_{|n|>N} \frac{1}{2\pi(1+n^2)^2}\Big|\sum_{m \in \mathbb{Z}}(1 + Z_m(kR)\overline{Z_n(kR)})c_m A_{mn}\Big|^2 \\
&\leq \sum_{n \in \mathbb{Z}} \frac{1}{2\pi(1+n^2)^2}\Big|\sum_{|m|>N}(1 + Z_m(kR)\overline{Z_n(kR)})c_m A_{mn}\Big|^2 \\
&\quad + \sum_{|n|>N} \frac{1}{2\pi(1+n^2)^2}\Big|\sum_{m \in \mathbb{Z}}(1 + Z_m(kR)\overline{Z_n(kR)})c_m A_{mn}\Big|^2 \\
&\leq 2 \sum_{|n|>N} \frac{1}{2\pi(1+n^2)^2}\Big|\sum_{m \in \mathbb{Z}}(1 + Z_m(kR)\overline{Z_n(kR)})c_m A_{mn}\Big|^2 \\
&\lesssim \sum_{|n|>N} \frac{1}{(2\pi)^2(1+n^2)^2}\Big(\sum_{m \in \mathbb{Z}} \frac{|(1 + Z_m(kR)\overline{Z_n(kR)})A_{mn}|^2}{(1+m^2)^2}\Big)\Big(\sum_{m \in \mathbb{Z}} 2\pi|c_m|^2(1+m^2)^2\Big) \\
&\lesssim \frac{1}{(2\pi)^2}\|\tilde{f}\|_2^2 \sum_{|n|>N} \frac{1}{(1+n^2)^2}\Big(\sum_{m \in \mathbb{Z}} \frac{(1 + |Z_m(kR)|^2)(1 + |\overline{Z_n(kR)}|^2)|A_{mn}|^2}{(1+m^2)^2}\Big) \\
&\lesssim \frac{1}{(2\pi)^2}\|\tilde{f}\|_2^2(\mathrm{meas}(\Gamma))^2\Big(\sum_{|n|>N} \frac{1}{1+n^2}\big(\sum_{m \in \mathbb{Z}} \frac{1}{1+m^2}\big)\Big) \\
&\lesssim \|\tilde{f}\|_2^2(\mathrm{meas}(\Gamma))^2\Big(\sum_{|n|>N} \frac{1}{n^2}\Big) \\
&\lesssim \|\tilde{f}\|_2^2(\mathrm{meas}(\Gamma))^2 \frac{1}{N^\rho}\Big(\sum_{n \in \mathbb{Z}} \frac{1}{n^{2-\rho}}\Big) \lesssim \|\tilde{f}\|_2^2(\mathrm{meas}(\Gamma))^2 \frac{1}{N^\rho}. \tag{3.10}
\end{aligned}$$

Therefore, (3.4) is obtained. $\qquad \square$

3.2. The projection method with regularization

The numerical method to deal with this Cauchy problem is divided into two parts. Firstly, the inversion of the compact operator equation (2.4) is obtained via a suitable projection method in conjunction with Hansen's L-curve method (see, e.g., [11]) for selecting the optimal regularization parameter. Then we reconstruct the wave field $u(x, y)$ from $\tilde{f}$.

Because of the compactness of K, we use Tikhonov's regularization method (see, e.g., [3, Chapter 4] and [19, Chapter 2]) to solve (2.4). For each $y = (f, g) \in \left[L^2(\Gamma) \right]^2$, determine $v^\alpha \in H^2(\partial B_R)$ that minimizes the Tikhonov functional

$$J_\alpha(v) := \left\| Kv - y \right\|^2_{\left[L^2(\Gamma) \right]^2} + \alpha \left\| v \right\|^2_2 \ \text{ for } \ v \in H^2(\partial B_R),$$

where $\alpha > 0$ is the regularization parameter. This minimum v^α is the unique solution of the normal equation

$$\alpha v^\alpha + K^* K v^\alpha = K^* y. \tag{3.11}$$

For the numerical treatment of the normal equation (3.11), we have to discretize this continuous problem and reduce it to a finite system of linear equations.

Let $\mathscr{T}_N \subset H^2(\partial B_R)$ be defined by

$$\mathscr{T}_N = \left\{ \sum_{|n| \leq N} c_n \mathrm{e}^{\mathrm{i}nt}; \ t \in [0, 2\pi] \right\}.$$

The projection operator $P_N : H^2(\partial B_R) \to \mathscr{T}_N$ is given by

$$P_N v = \sum_{|n| \leq N} a_n \mathrm{e}^{\mathrm{i}nt} \ , \quad t \in [0, 2\pi], \ \text{ for } v = \sum_{n \in \mathbb{Z}} a_n \mathrm{e}^{\mathrm{i}nt} \in H^2(\partial B_R).$$

It is evident that P_N is an orthogonal projection operator onto $\mathscr{T}_N$. Then an obvious method to solve (3.11) is the following: Find $v_N^\alpha \in \mathscr{T}_N$, such that

$$P_N(\alpha v_N^\alpha + K^* K v_N^\alpha) = P_N K^* y. \tag{3.12}$$

It is the projection method with regularization for solving the compact operator equation (2.4). The existence and uniqueness of $v_N^\alpha \in \mathscr{T}_N$ follow easily since $\mathscr{T}_N$ is finite-dimensional and $\alpha I + K^* K$ is one-to-one. In the following part, we will give the convergence analysis of the projection method.

For any $v_N \in \mathscr{T}_N$, we have

$$\langle (\alpha I + P_N K^* K) v_N, v_N \rangle_2 = \alpha \langle v_N, v_N \rangle_2 + \langle Kv_N, Kv_N \rangle \geq \alpha \left\| v_N \right\|^2_2. \tag{3.13}$$

Hence $\alpha I + P_N K^* K$ coercive on $\mathscr{T}_N$ and

$$\left\| (\alpha I + P_N K^* K)^{-1} \big|_{\mathscr{T}_N} \right\| \leq \frac{1}{\alpha}. \tag{3.14}$$

Combining

$$P_N(\alpha v^\alpha + K^* K v^\alpha) = P_N K^* y \tag{3.15}$$

with (3.12) yields

$$(\alpha I + P_N K^* K)(P_N v^\alpha - v_N^\alpha) = P_N K^* K(P_N v^\alpha - v^\alpha).$$

Thus

$$\left\|P_N v^\alpha - v_N^\alpha\right\|_2 \lesssim \frac{1}{\alpha}\left\|P_N v^\alpha - v^\alpha\right\|_2, \tag{3.16}$$

since $P_N K^* K$ is bounded.

We summarize these results in the following theorem.

Theorem 3.3. *The solution v_N^α of* (3.12) *converges to v^α which is the solution of* (3.11), *and the following error estimate holds*:

$$\left\|v^\alpha - v_N^\alpha\right\|_2 \lesssim (1 + \frac{1}{\alpha}) \inf_{v_N \in \mathscr{T}_N} \left\|v_N - v^\alpha\right\|_2. \tag{3.17}$$

Using Theorem 3.3 and the convergence of Tikhonov's regularization method (see, e.g., [19, Chapter 2]), we obtain the following result.

Theorem 3.4. *Let $y \in K\big(H^2(\partial B_R)\big)$. For $\varepsilon > 0$ there exist $N = N(\alpha, \varepsilon)$ and*

$$v_N^\alpha = \sum_{|n| \leqslant N} c_n \mathrm{e}^{int}, \tag{3.18}$$

such that

$$\|v_N^\alpha - \widetilde{f}\|_2 < \varepsilon. \tag{3.19}$$

Proof. Given $\varepsilon > 0$, there is a regularization parameter α satisfying

$$\|v^\alpha - \widetilde{f}\|_2 < \varepsilon/2,$$

where v^α is the solution of equation (3.11). By Theorem 3.3 there exists $N = N(\alpha, \varepsilon)$ such that

$$\|v_N^\alpha - v^\alpha\|_2 < \varepsilon/2,$$

where v_N^α is the solution of (3.12). Then from the triangle inequality, we conclude that

$$\|v_N^\alpha - \widetilde{f}\|_2 \leq \|v^\alpha - \widetilde{f}\|_2 + \|v^\alpha - v_N^\alpha\|_2 < \varepsilon,$$

which is the desired estimate (3.19). $\qquad\square$

In practice, the right-hand side y of the operator equation is often perturbed by the measurement error. Therefore we assume that we know $\delta > 0$ and $y^\delta \in \big(L^2(\Gamma)\big)^2$ with

$$\|y - y^\delta\|_{\left[L^2(\Gamma)\right]^2} \leqslant \delta.$$

Then we determine $v_N^{\alpha,\delta}$ such that

$$P_N(\alpha v_N^{\alpha,\delta} + K^* K v_N^{\alpha,\delta}) = P_N K^* y^\delta. \tag{3.20}$$

Subtracting (3.15) yields

$$(\alpha I + P_N K^* K)(P_N v^\alpha - v_N^{\alpha,\delta}) = P_N K^* K(P_N v^\alpha - v^{\alpha,\delta}) + P_N K^* K(y - y^\delta).$$

Thus we have

$$\left\|P_N v^\alpha - v_N^{\alpha,\delta}\right\|_2 \lesssim \frac{1}{\alpha}\left\|P_N v^\alpha - v^\alpha\right\|_2 + \frac{1}{\alpha}\left\|y - y^\delta\right\|_{\left[L^2(\Gamma_1)\right]^2}.$$

On account of the above deduction, we conclude that the numerical method is stable for a given regularization parameter α.

The solution v_N^α of the projection method (3.12) is also characterized by

$$\langle(\alpha I + P_N K^* K)v_N^\alpha, v\rangle_2 = \langle K^* y, v\rangle_2, \quad \text{for all } v \in \mathscr{T}_N. \tag{3.21}$$

Then choosing the basis $\{v_n = \mathrm{e}^{int}; \ 0 \le |n| \le N\}$ of $\mathscr{T}_N$ leads to the finite system for the coefficients of $v_N^\alpha = \sum\limits_{|n| \leqslant N} c_n \mathrm{e}^{int}$:

$$\sum_{|n| \leqslant N} c_n(\alpha\langle v_n, v_j\rangle_2 + \langle K v_n, K v_j\rangle) = \langle y, K v_j\rangle \ \text{ for } \ |j| \le N,$$

where

$$K v_n = \left(\mathrm{e}^{int}\Big|_\Gamma, Z_n(kR)\mathrm{e}^{int}\Big|_\Gamma\right) \quad \text{for } \ 0 \le |n| \le N.$$

We observe that the projection method with $\alpha = 0$ is just the least squares method. In the case that the Cauchy problem is ill-posed, the smallest eigenvalue of $P_N K^* K P_N$ decreases rapidly as N tends to infinity. The solution of the least squares method is therefore useless if N is large. But the numerical solution of the Cauchy problem, which is obtained via the projection method in conjunction with Hansen's L-curve criterion (see, e.g., [11]) for selecting the optimal regularization parameter, is accurate and effective. In section 5, we will show several numerical examples to demonstrate the effectiveness of our method.

4. The Three-Dimensional Case

In this section, we assume that k^2 is not a Dirichlet eigenvalue of $-\Delta$ in B_R. Let $\| \cdot \|_s$ and $\langle\cdot, \cdot\rangle_s$ denote the norm and inner product in the space $H^s(\partial B_R)$, respectively. The inner product in the space $[L^2(\Gamma)]^2$ is also given by

$$\langle F, G\rangle = \int_\Gamma \left(f_1\overline{g_1} + f_2\overline{g_2}\right)\mathrm{d}s.$$

For $\tilde{f} \in H^3(\partial B_R)$ given by

$$\tilde{f} = \sum_{n=0}^\infty \sum_{m=-n}^n c_n^m Y_n^m(\theta, \phi),$$

we have

$$\Lambda\tilde{f} = \sum_{n=0}^\infty \sum_{m=-n}^n c_n^m z_n(kR)Y_n^m(\theta, \phi), \quad \text{with} \ \ z_n(kR) = \frac{n}{R} - \frac{kh_{n+1}(kR)}{h_n(kR)}, \tag{4.1}$$

where h_n are the nth-order spherical Hankel functions of the first kind and Y_n^m, $m = -n, \cdots, n$ are the corresponding spherical harmonics. The coefficients are given by $c_n^m = \langle\tilde{f}, Y_n^m\rangle_0$. The relations between the spherical Hankel functions and the Hankel functions are

$$h_n(x) = \sqrt{\frac{\pi}{2x}}H_{n+\frac{1}{2}}(x)$$

(see, e.g., [3, Chapter 2]). Therefore we have $h_n(kR) \ne 0$ for any $n \in \mathbb{Z}$, $R > 0$ (see, e.g., [5]). It is reasonable that $h_n(kR)$ are in the denominator. Then the radiation solution to the Helmholtz

equation in the exterior of B_R, which satisfies the Dirichlet boundary condition $u = \tilde{f}$ on ∂B_R, is given by

$$u(r, \theta, \phi) = \sum_{n=0}^{\infty} \sum_{m=-n}^{n} \frac{c_n^m}{h_n(kR)} h_n(kr) Y_n^m(\theta, \phi), \quad \theta \in [0, \pi], \quad \phi \in [0, 2\pi]. \tag{4.2}$$

Hence, we only need to solve the following problem.

Problem 3. *Given $f, g \in L^2(\Gamma)$, find a function $\tilde{f} = \sum\limits_{n=0}^{\infty} \sum\limits_{m=-n}^{n} c_n^m Y_n^m(\theta, \phi) \in H^3(\partial B_R)$ satisfying*

$$\tilde{f} = f, \quad \Lambda \tilde{f} = g, \quad on \ \Gamma. \tag{4.3}$$

In the case that the inner product in the space $H^2(\partial B_R)$ is defined by the Fourier coefficients of $\tilde{f}$, the inversion of the compact operator equation is transformed into the linear algebraic equations for the Fourier coefficients of $\tilde{f}$ in the two-dimensional case. We also want to reduce the compact operator equation to the linear algebraic equations for the coefficients of $\tilde{f}$ with respect to the spherical wave functions in the three-dimensional case. But we need to compute the higher-order derivatives of the spherical wave functions. However, the higher-order derivatives are not easy to get and so they are difficult in the numerical calculations. We overcome this difficulty by incorporating acoustic single-layer potential.

We first review some properties of acoustic single-layer potential which are used in the following deduction. Given an integrable function φ, the integral

$$(S\varphi)(x) := \int_{\partial B_R} \Phi(x, y) \varphi(y) \mathrm{d}s(y), \quad x \in \partial B_R, \tag{4.4}$$

is called acoustic single-layer potential with density φ. Here Φ is the free space radiation fundamental solution to the Helmholtz equation in $\mathbb{R}^3$. We recall that

$$\Phi(x, y) = \frac{1}{4\pi} \frac{e^{ik|x-y|}}{|x-y|}, \quad x \neq y.$$

Lemma 4.1. *Let $s \geq 1$. The operator S is bounded from $H^{s-1}(\partial B_R)$ into $H^s(\partial B_R)$.*

Lemma 4.2. *Assume k^2 is not a Dirichlet eigenvalue of $-\Delta$ in B_R. We have*

$$S Y_n^m = a_n(kR) Y_n^m, \tag{4.5}$$

where $a_n(kR) = ikR^2 j_n(kR) h_n(kR)$. $j_n(kR)$ are the spherical Bessel functions of order n.

For a proof, we refer to the references [2, Chapter 2] and [3, Chapter 3].

From [5, Lemma 2.1] and the assumption of Lemma 4.2 we have that $a_n(kR) \neq 0$ for any $n \in \mathbb{Z}$, $R > 0$.

By (4.5), we get that

$$S^3 Y_n^m(\hat{x}) = (a_n(kR))^3 Y_n^m(\hat{x}), \tag{4.6a}$$

$$\Lambda S^3 Y_n^m(\hat{x}) = (a_n(kR))^3 z_n(kR) Y_n^m(\hat{x}). \tag{4.6b}$$

Hence, the operator $T : L^2(\partial B_R) \to [L^2(\Gamma)]^2$ given by

$$T\varphi = K S^3 \varphi = \left(S^3 \varphi \Big|_{\Gamma}, \Lambda S^3 \varphi \Big|_{\Gamma} \right), \quad \text{for } \varphi \in L^2(\partial B_R) \tag{4.7}$$

is well-defined. The Cauchy problem is transformed into the following compact operator equation:

Problem 4. *Given $f, g \in L^2(\Gamma)$, find a function $\varphi = \sum_{n=0}^{\infty} \sum_{m=-n}^{n} a_n^m Y_n^m(\theta, \phi) \in L^2(\partial B_R)$, such that*

$$T\varphi = (f, g), \quad \text{for } \varphi \in L^2(\partial B_R). \tag{4.8}$$

Then the solution of (2.4) has the form $\tilde{f} = S^3 \varphi$.

4.1. Ill-posedness of the problem

In this subsection, we will analyze the asymptotic behaviors of singular values of the compact operator T. The following results are proved in much the same way as the two-dimensional case.

Theorem 4.1. $T : L^2(\partial B_R) \to [L^2(\Gamma)]^2$ *is a compact operator.*

Proof. Since $K : H^3(\partial B_R) \to H^3(\Gamma) \times H^2(\Gamma)$ and $S^3 : L^2(\partial B_R) \to H^3(\partial B_R)$ are bounded, we get $T : L^2(\partial B_R) \to H^3(\Gamma) \times H^2(\Gamma)$ is bounded. Then using the compactness of the imbedding operator from $H^3(\Gamma) \times H^2(\Gamma)$ into $[L^2(\Gamma)]^2$, we yield the conclusion. $\square$

Theorem 4.2. *For the eigenvalues $\mu_n(T^*T)$ of T^*T, we have the estimation*

$$\mu_n(T^*T) \lesssim \frac{1}{n^{\frac{\rho}{3}}} \text{meas}(\Gamma), \quad n \to \infty, \tag{4.9}$$

where $0 < \rho < 1$ and T^* denotes the adjoint operator of T.

Proof. Given

$$\tilde{f} = \sum_{n=0}^{\infty} \sum_{m=-n}^{n} a_n^m Y_n^m \in L^2(\partial B_R) \text{ and } \tilde{h} = \sum_{n=0}^{\infty} \sum_{m=-n}^{n} d_n^m Y_n^m \in L^2(\partial B_R),$$

we have that

$$\langle T\tilde{f}, T\tilde{h} \rangle$$

$$= \left\langle \sum_{n=0}^{\infty} \sum_{m=-n}^{n} a_n^m (a_n(kR))^3 Y_n^m, \sum_{n=0}^{\infty} \sum_{m=-n}^{n} d_n^m (a_n(kR))^3 Y_n^m \right\rangle_{L^2(\Gamma)}$$

$$+ \left\langle \sum_{n=0}^{\infty} \sum_{m=-n}^{n} a_n^m (a_n(kR))^3 z_n(kR) Y_n^m, \sum_{n=0}^{\infty} \sum_{m=-n}^{n} d_n^m (a_n(kR))^3 z_n(kR) Y_n^m \right\rangle_{L^2(\Gamma)}$$

$$= \sum_{n=0}^{\infty} \sum_{m=-n}^{n} \overline{d_n^m (a_n(kR))^3} \left(\sum_{n'=0}^{\infty} \sum_{m'=-n'}^{n'} a_{n'}^{m'} (a_{n'}(kR))^3 (1 + z_{n'}(kR)\overline{z_n(kR)}) \langle Y_{n'}^{m'}, Y_n^m \rangle_{L^2(\Gamma)} \right).$$

Let $A_{nn'}^{mm'} = \langle Y_n^m, Y_{n'}^{m'} \rangle_{L^2(\Gamma)}$ and

$$\hat{f} = \sum_{n=0}^{\infty} \sum_{m=-n}^{n} \overline{(a_n(kR))^3} \left(\sum_{n'=0}^{\infty} \sum_{m'=-n'}^{n'} a_{n'}^{m'} (a_{n'}(kR))^3 (1 + z_{n'}(kR)\overline{z_n(kR)}) A_{n'n}^{m'm} \right) Y_n^m.$$

It is obvious that $|A_{nn'}^{mm'}| < \text{meas}(\Gamma)$. From the above deduction and the relation

$$\langle \hat{f}, \tilde{h} \rangle_0 = \langle T\tilde{f}, T\tilde{h} \rangle = \langle T^*T\tilde{f}, \tilde{h} \rangle_0$$

for all $\tilde{h} \in L^2(\partial B_R)$, we obtain that $\hat{f} = T^*T\tilde{f}$.

Introducing

$$A_N \tilde{f} = \sum_{n=0}^{N} \sum_{m=-n}^{n} \overline{(a_n(kR))^3} \Big(\sum_{n'=0}^{N} \sum_{m'=-n'}^{n'} a_{n'}^{m'} (a_{n'}(kR))^3 (1 + z_{n'}(kR)\overline{z_n(kR)}) A_{n'n}^{m'm} \Big) Y_n^m$$

we have

$$A_N(L^2(\partial B_R)) \subset \mathrm{span}\Big\{ Y_n^m;\ m = -n, \cdots n, 0 \le n \le N \Big\}$$

with

$$\dim A_N(L^2(\partial B_R)) \le (N+1)^2.$$

It means that A_N has at most $(N+1)^2$ non-vanishing eigenvalues. The min-max principle on the self-adjoint operator (see, e.g., [25, Chapter 13]) gives the relation

$$\mu_{(N+1)^2+1}(T^*T) \le \mu_{(N+1)^2+1}(A_N) + \mu_1(T^*T - A_N)$$
$$\le 0 + \|T^*T - A_N\|_0. \tag{4.10}$$

From the asymptotic behaviors of

$$j_n(t) = \frac{t^n}{(2n+1)!!}\Big(1 + \mathcal{O}(\frac{1}{n})\Big) \quad \text{and} \quad h_n(t) = \frac{(2n-1)!!}{\mathrm{i}t^{n+1}}\Big(1 + \mathcal{O}(\frac{1}{n})\Big), \quad n \to \infty$$

(see, e.g., [3, Chapter 2]), we obtain that

$$|a_n(kR)| \sim \frac{1}{2n+1} \quad \text{and} \quad |z_n(kR)| \sim n, \quad n \to \infty, \tag{4.11}$$

where $A \sim B$ means that $c_1 B \le A \le c_2 B$ with constants $c_1, c_2 > 0$. From the Cauchy inequality, we estimate

$$\|(T^*T - A_N)\tilde{f}\|_0^2$$

$$= \sum_{n=0}^{N} \sum_{m=-n}^{n} |\overline{(a_n(kR))^3}|^2 \Big| \sum_{n'>N}^{\infty} \sum_{m'=-n'}^{n'} a_{n'}^{m'}(a_{n'}(kR))^3(1 + z_{n'}(kR)\overline{z_n(kR)})A_{n'n}^{m'm} \Big|^2$$

$$+ \sum_{n>N}^{\infty} \sum_{m=-n}^{n} |\overline{(a_n(kR))^3}|^2 \Big| \sum_{n'=0}^{\infty} \sum_{m'=-n'}^{n'} a_{n'}^{m'}(a_{n'}(kR))^3(1 + z_{n'}(kR)\overline{z_n(kR)})A_{n'n}^{m'm} \Big|^2$$

$$\lesssim \sum_{n>N}^{\infty} \sum_{m=-n}^{n} |\overline{(a_n(kR))^3}|^2 \Big(\sum_{n'=0}^{\infty} \sum_{m'=-n'}^{n'} |a_{n'}^{m'}|^2 \Big)$$

$$\times \Big(\sum_{n'=0}^{\infty} \sum_{m'=-n'}^{n'} |(a_{n'}(kR))^3(1 + z_{n'}(kR)\overline{z_n(kR)})A_{n'n}^{m'm}|^2 \Big)$$

$$\lesssim \|\tilde{f}\|_0^2 (\mathrm{meas}(\Gamma))^2 \sum_{n>N}^{\infty} \sum_{m=-n}^{n} |\overline{(a_n(kR))^3}|^2$$

$$\times \Big(\sum_{n'=0}^{\infty} \sum_{m'=-n'}^{n'} |(a_{n'}(kR))^3|^2(1 + |z_{n'}(kR)|^2)(1 + |\overline{z_n(kR)}|^2) \Big)$$

$$\lesssim \|\tilde{f}\|_0^2 (\mathrm{meas}(\Gamma))^2 \sum_{n>N}^{\infty} \sum_{m=-n}^{n} \frac{1}{(2n+1)^6} \Big(\sum_{n'=0}^{\infty} \sum_{m'=-n'}^{n'} \frac{(1+n'^2)(1+n^2)}{(2n'+1)^6} \Big)$$

$$\lesssim \|\tilde{f}\|_0^2 (\text{meas}(\Gamma))^2 \sum_{n>N}^{\infty} \sum_{m=-n}^{n} \frac{1}{(2n+1)^4} \Big(\sum_{n'=0}^{\infty} \sum_{m'=-n'}^{n'} \frac{1}{(2n'+1)^4} \Big)$$

$$\lesssim \|\tilde{f}\|_0^2 (\text{meas}(\Gamma))^2 \sum_{n>N}^{\infty} \sum_{m=-n}^{n} \frac{1}{(2n+1)^4} \lesssim \|\tilde{f}\|_0^2 (\text{meas}(\Gamma))^2 \sum_{n>N}^{\infty} \frac{1}{(2n+1)^3}$$

$$\lesssim \|\tilde{f}\|_0^2 (\text{meas}(\Gamma))^2 \frac{1}{N^{2\rho}} \sum_{n>0}^{\infty} \frac{1}{n^{3-2\rho}} \lesssim \|\tilde{f}\|_0^2 (\text{meas}(\Gamma))^2 \frac{1}{N^{2\rho}}. \tag{4.12}$$

Therefore, we yield

$$\mu_{N^3}(T^*T) \leq \mu_{(N+1)^2+1}(T^*T) \lesssim (\text{meas}(\Gamma)) \frac{1}{N^\rho}, \quad \text{for } N > 3,$$

(4.9) is satisfied. $\hfill\square$

4.2. The projection method with regularization

We use Tikhonov's regularization method to solve (4.8) as section 3. Let $y = (f, g) \in \left[L^2(\Gamma)\right]^2$. We determine $v^\alpha \in L^2(\partial B_R)$ that minimizes the Tikhonov functional

$$J_\alpha(v) := \|Tv - y\|_{\left[L^2(\Gamma)\right]^2}^2 + \alpha \|v\|_0^2 \quad \text{for } v \in L^2(\partial B_R), \tag{4.13}$$

where $\alpha > 0$ is the regularization parameter. This minimum v^α is the unique solution of the normal equation

$$\alpha v^\alpha + T^*T v^\alpha = T^* y. \tag{4.14}$$

Next, we use the projection method with regularization to solve (4.14). Let $\mathscr{T}_N \subset L^2(\partial B_R)$ be defined by

$$\mathscr{T}_N = \Big\{ \sum_{n \leq N} \sum_{m=-n}^{n} a_n^m Y_n^m \Big\}.$$

The corresponding projection operator $P_N : L^2(\partial B_R) \to \mathscr{T}_N$ is given by

$$P_N v = \sum_{n=0}^{N} \sum_{m=-n}^{n} a_n^m Y_n^m,$$

for $v = \sum_{n=0}^{\infty} \sum_{m=-n}^{n} a_n^m Y_n^m$. Then find $v_N^\alpha \in \mathscr{T}_N$, such that

$$P_N(\alpha v_N^\alpha + T^*T v_N^\alpha) = P_N T^* y. \tag{4.15}$$

The solution of (4.15) is characterized by

$$\langle (\alpha I + P_N T^*T) v_N^\alpha, v \rangle_0 = \langle T^* y, v \rangle_0, \quad \text{for all } v \in \mathscr{T}_N. \tag{4.16}$$

Then choosing the basis

$$\Big\{ v_n^m = \frac{Y_n^m}{(a_n(kR))^3}; \ |m| \leq n, \ 0 \leq n \leq N \Big\} \tag{4.17}$$

of $\mathscr{T}_N$ leads to the finite system for the coefficients $v_N^\alpha = \sum\limits_{n=0}^{N} \sum\limits_{m=-n}^{n} \dfrac{c_n^m}{(a_n(kR))^3} Y_n^m$:

$$\sum_{n=0}^{N} \sum_{m=-n}^{n} \left(\frac{\alpha}{(a_n(kR))^3 \overline{(a_{n'}(kR))^3}} \langle Y_n^m, Y_{n'}^{m'} \rangle_0 + \langle TY_n^m, TY_{n'}^{m'} \rangle \right) c_n^m$$
$$= \langle y, TY_{n'}^{m'} \rangle \quad \text{for } |m'| \le n', \ 0 \le n' \le N, \tag{4.18}$$

where

$$Tv_n^m = \left(Y_n^m \Big|_\Gamma, z_n(kR) Y_n^m \Big|_\Gamma \right) \quad \text{for } |m| \le n, \ 0 \le n \le N.$$

Using Lemma 4.2, the approximate solution of (2.4) is given by

$$\tilde{f}_N^\alpha = S^3 v_N^\alpha = \sum_{n=0}^{N} \sum_{m=-n}^{n} c_n^m Y_n^m. \tag{4.19}$$

The convergence analysis of the numerical method in the three-dimensional case is similar to the two-dimensional case.

5. Numerical Results and Discussions

In this section, some numerical tests are presented to show the feasibility of the projection method with regularization. The implementation of these numerical examples is based on MATLAB. Cauchy data are created using a point source $G(x, y)$, which is enclosed in the ball B_R of radius R. The input data with an additive random noise are given on Γ, which is a part of the boundary ∂B_R. The relative noise level is δ. Let f^δ, g^δ denote the noise data for the wave field and its normal derivative respectively. Then we have

$$\frac{\|f^\delta - f\|_{L^2(\Gamma)}}{\|f\|_{L^2(\Gamma)}} \le \delta \quad \text{and} \quad \frac{\|g^\delta - g\|_{L^2(\Gamma)}}{\|g\|_{L^2(\Gamma)}} \le \delta.$$

For $r \ge R$, we reconstruct the wave field on the sphere ∂B_r. Let F denote the exact value of G and Num denote the numerical approximate solution of G on ∂B_r. The relative error between them is given by

$$Error = \frac{\|Num - F\|_{L^2(\partial B_r)}}{\|F\|_{L^2(\partial B_r)}}. \tag{5.1}$$

We show the absolute values of G and Num in the following figures. The choice of the regularization parameter α is based on the L-curve criterion (see, e.g., [11]).

In the two-dimensional case, let

$$G(x, y) = \frac{\mathrm{i}}{4} H_0(k|x - y|) \tag{5.2}$$

be a point source located at $y=(1, 2)^T$. The input data are given on

$$\Gamma := \left\{ (R \cos t, R \sin t); t \in I \right\}.$$

Denote $\Gamma_r := \{(r \cos t, r \sin t); \ t \in I\}$. Set $R = 20$, $r = 22$.

In the three-dimensional case, let

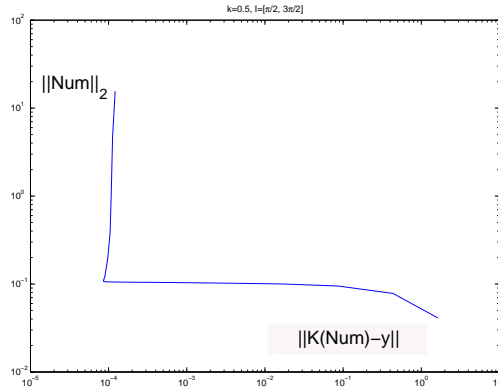$$G(x, y) = \frac{\mathrm{e}^{\mathrm{i}k|x-y|}}{4\pi|x - y|} \tag{5.3}$$

Fig. 5.1. Example 5.1: The L-curve obtianed for $\delta = 0$, $k = 0.5$ and $I = [\pi/2, 3\pi/2]$.

with $y = (1, 2, 3)^T$. The input data are given on

$$\Gamma := \Big\{ (R\sin\theta\cos\varphi, R\sin\theta\sin\varphi, R\cos\theta);\ \theta \in I_\theta, \varphi \in I_\varphi \Big\}.$$

Denote

$$\Gamma_r := \Big\{ (r\sin\theta\cos\varphi, r\sin\theta\sin\varphi, r\cos\theta);\ \theta \in I_\theta, \varphi \in I_\varphi \Big\}.$$

We choose $R = 32$, $r = 35$.

First we compare the least squares method with the projection method with regularization in the first example. The relations between the ill-posedness of the Cauchy problem and the measure of Γ are discussed.

Example 5.1. (2-D) Let $\delta = 0$, $N = 20$. We choose $k = 0.5, 1, 3$. The input data are given on a single segment with different locations over a sphere. Table 5.1 presents the relative errors of the least squares method and the projection method in conjunction with the L-curve criterion. The L-curve obtained for the Cauchy problem given by $k = 0.5$, $I = [\pi/2, 3\pi/2]$ is shown in Fig. 5.1.

Table 5.1: The relative errors of the least squares method and the projection method

I	$[0, 2\pi]$	$[\pi/4, 7\pi/4]$	$[\pi/2, 3\pi/2]$	$[3\pi/4, 5\pi/4]$
$k = 0.5$, $\alpha = 0$	1.4227e-5	3.6311	1.0752e+4	2.5293e+4
$k = 0.5$, $\alpha \neq 0$		0.0275	0.1083	0.3581
$k = 1$, $\alpha = 0$	1.9068e-5	115.1908	5.8652e+5	1.6637e+4
$k = 1$, $\alpha \neq 0$		0.0942	0.3766	0.6408
$k = 3$, $\alpha = 0$	1.9532e-5	363.3782	2.7301e+3	3.4812e+4
$k = 3$, $\alpha \neq 0$		0.7949	1.4066	1.7626

Table 5.1 indicates that the least squares method for $N = 20$ is unstable unless the input data are provided over the surface ∂B_R. The condition number of the matrix corresponding to the least squares method increases rapidly as the measure of Γ tends to zero. Therefore, if the input data are given on a portion of the boundary, we use the numerical method with regularization to solve the Cauchy problem. The results demonstrate that the projection method

with regularization is more consistent, reliable and accurate. The numerical algorithm is especially effective for the small wave number. However, as the measure of Γ decreases further, the effectiveness of the numerical method becomes hindered. If the input data are given on a single segment, a considerable extent of the segment is needed in order to achieve the wave field reconstruction with acceptable accuracy. In Fig. 5.1, we can clearly see the "corner" of the corresponding L-curve. However, it is hard to judge whether the errors in the results are due to inappropriate choice of the regularization parameter, or inherent lack of information. Therefore, we manually tune the regularization parameter nearby the "corner" of the corresponding L-curve. We choose the parameter α that gives a minimal L^2-norm of $Num - G$ among all the regularization parameters, which were chosen.

Next the effect of the reconstructed solution using the input data from two segments with different locations over a sphere is discussed in Example 5.2.

Example 5.2. (2-D) Set $\delta = 0$, $N = 20$. Let $k = 0.5, 1, 3$. In the first case, the input data are given on $I_1 = [0, \pi]$ and $I_2 = [0, \pi/2] \cup [\pi, 3\pi/2]$, which are $1/2$ of the circumference of the circle. Fig. 5.2 shows the results for these different input data. When the input date are given on I_2, the numerical solution is more accurate for $k = 0.5$ and $k = 1$. In the second case, the input data are given on $[0, \pi/2]$, $[0, \pi/4] \cup [\pi/2, 3\pi/4]$ and $[0, \pi/4] \cup [\pi, 5\pi/4]$. Table 5.2 and Table 5.3 present the relative errors for the two cases, respectively. For $k = 0.5$, although the input data are given on $[0, \pi/4] \cup [\pi, 5\pi/4]$, which is only $1/4$ of the circumference of the circle, the relative error, which is 0.1395, is smaller than the case that the input data are given on $I_1 = [0, \pi]$, for which the relative error is 0.1582. Here we observe the same effect as [30], i.e., if the input data are available on multiple segments over a sphere, a better accuracy of the reconstructed solution will be obtained, especially when the segments are on the opposite sides (see, e.g., [30]).

Example 5.3. (2-D) In this example, the effect of the random noisy is investigated. The input data are given on $[0, 3\pi/4] \cup [\pi, 7\pi/4]$. Set $N = 20$, $\delta = 1\%$, 0.1%. Let $k = 0.5$, 1. The reconstructed wave field from the projection method is compared with the analytical solution in Fig. 5.3 for different noisy levels. Fig. 5.3(A) demonstrate that the accuracy of the reconstructed solution with the noisy level up to 1% is overall acceptable for $k = 0.5$. For $k = 1$,
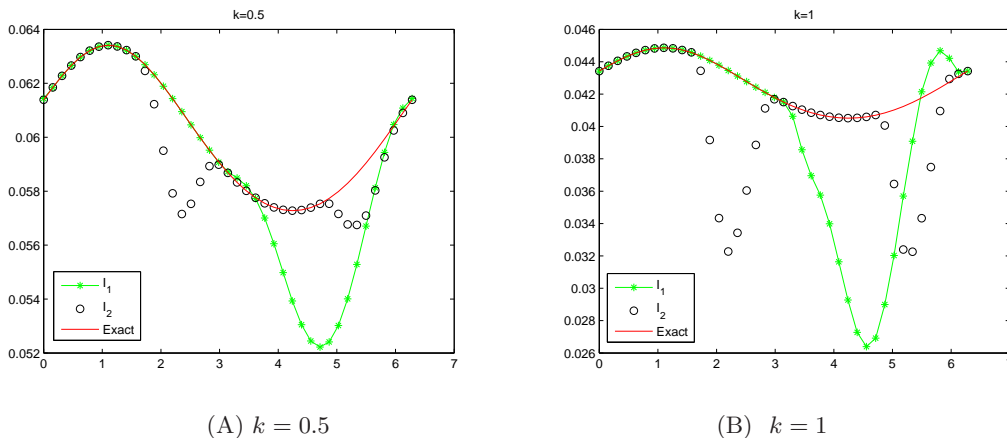

(A) $k = 0.5$ (B) $k = 1$

Fig. 5.2. Example 5.2: numerical results with different input.

Table 5.2: 1/2 Circumference of the Circle

I	$[0, \pi]$	$[0, \pi/2] \cup [\pi, 3\pi/2]$
$k = 0.5$	0.1582	0.0234
$k = 1$	0.3499	0.1220
$k = 3$	1.5381	0.8128

Table 5.3: 1/4 Circumference of the Circle

I	$[0, \pi/2]$	$[0, \pi/4] \cup [\pi/2, 3\pi/4]$	$[0, \pi/4] \cup [\pi, 5\pi/4]$
$k = 0.5$	0.4931	0.3568	0.1395
$k = 1$	0.9229	0.8136	0.4705
$k = 3$	1.3400	1.8715	1.0880

the numerical solution is acceptable on Γ_r. From Fig. 5.3, we observe that the accuracy of the numerical results for $\delta = 1\%$ is practically the same for $\delta = 0.1\%$. Therefore, we conclude that the numerical algorithm is less sensitive to the random noises.

From Figs. 5.2 and 5.3, we see that the numerical solutions are more accurate on Γ_r than any other places and the results are less dependable on the length of the segments on which the input data are given. Therefore we will only show the results on Γ_r in Example 5.4.

Example 5.4. (2-D) Set $N = 100$, $\delta = 0$. In the first case, let $k = 10$. The input data are given on $[0, \pi]$. The numerical solution which is compared with the analytical solution is shown in Fig. 5.4(A). The results of $k = 30$ are shown in Fig. 5.4(B), where the input data are given on $[0, 3\pi/2]$. We observe that the results are also accurate on Γ_r for the large wave number. Therefore the projection method with regularization is effective and stable.

For the three-dimensional case, the results are shown on the curve

$$\gamma : = \left\{ (r \sin \theta \cos \varphi, r \sin \theta \sin \varphi, r \cos \theta); \ \theta = 1.3, \varphi \in [0, 2\pi] \right\}.$$
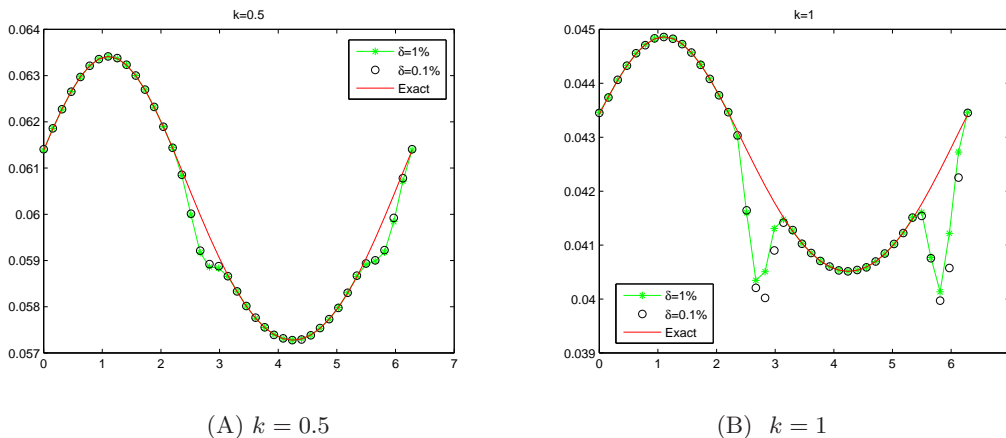

(A) $k = 0.5$ (B) $k = 1$

Fig. 5.3. comparison between the reconstructed wave field and the exact solution.
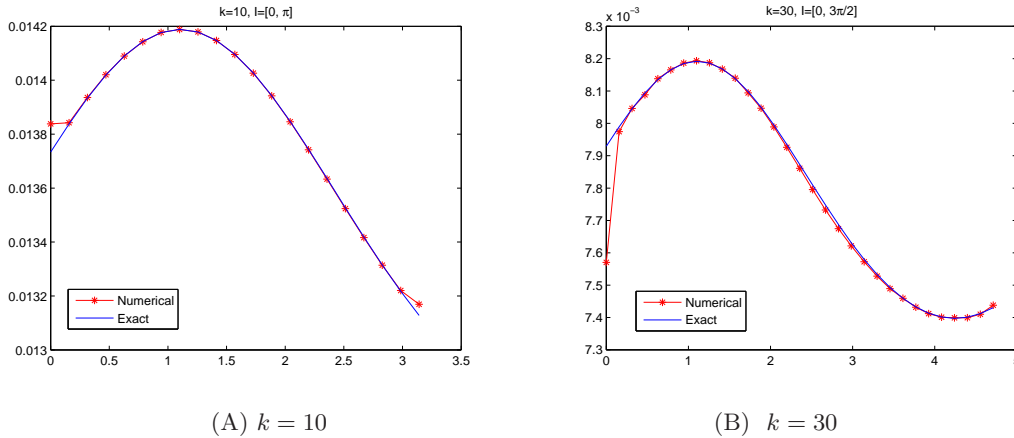
(A) $k = 10$ (B) $k = 30$

Fig. 5.4. Example 5.4: comparison between the numerical and the analytical solution.

Example 5.5. (3-D) Set $N = 10$, $\delta = 0$. Let $k = 0.2$, 1. In the first case, the input data are given on $I_1 = I_\theta^1 \times I_\varphi^1$, where $I_\theta^1 = [0, \pi]$ and $I_\varphi^1 = [0, 3\pi/2]$. In the second case, the input data are given on $I_2 = I_\theta^2 \times I_\varphi^2$, where $I_\theta^2 = [0, \pi]$ and $I_\varphi^2 = [0, 3\pi/4] \cup [\pi, 7\pi/4]$. The reconstructed wave field, which is compared with the analytical solution, is shown in Fig. 5.5. We note that the numerical solution for I_2 is more accurate than I_1, where the input data are given on two opposite segments for I_2. We observe the same behaviors as the two-dimensional case, i.e., the numerical results are more accurate when the input data are given on the opposite segments.

Example 5.6. (3-D) Set $N = 10$, $\delta = 1\%$, 0.1%. Let $k = 0.2$, 1. The input data with an additive random noise are given on I_2. Fig. 5.6(A) presents the results for $k = 0.2$. The results of $k = 1$ are shown in Fig. 5.6(B). We see that with up to 1% random noises the numerical solution agrees with the analytical solution reasonably well. The numerical algorithm is therefore stable.

Example 5.7. (3-D) Let $k = 3$. The input data are given on I_1. The results of the reconstructed wave field on Γ_r for $\delta = 0$ are shown in Fig. 5.7(a). Fig. 5.7(b) presents the analytical
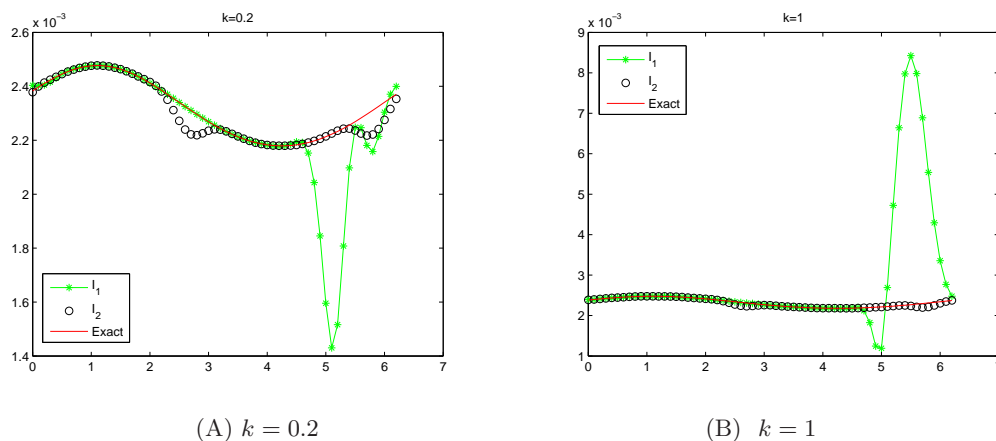

(A) $k = 0.2$ (B) $k = 1$

Fig. 5.5. Example 5.5: the reconstructed wave field and exact solution.

(A) $k = 0.2$ (B) $k = 1$

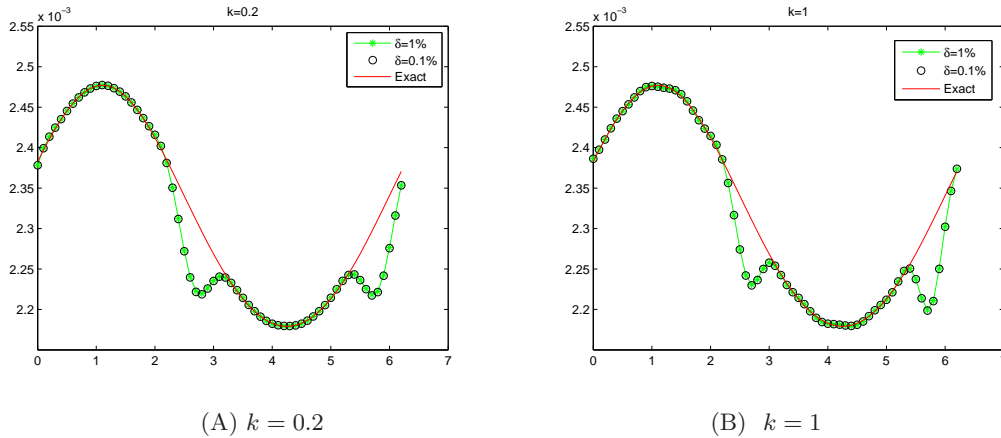Fig. 5.6. Example 5.6: numerical results with different noises.

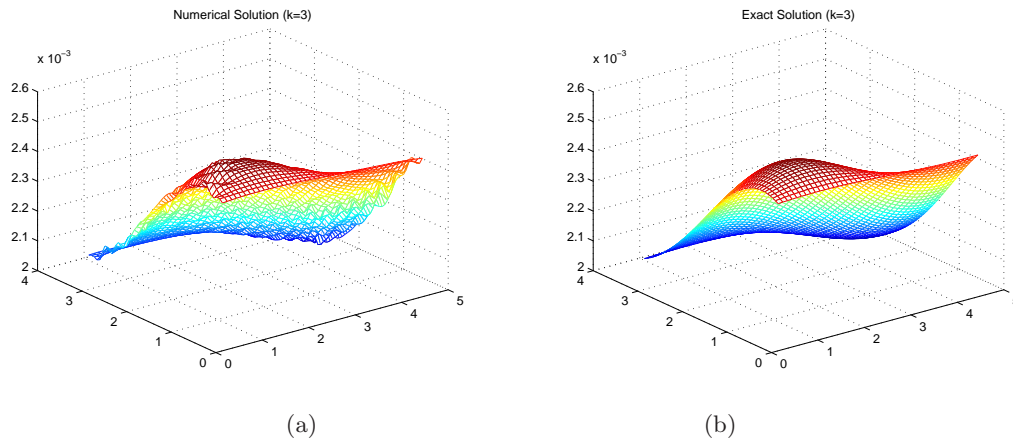(a)   (b)

Fig. 5.7. Example 5.7: contour of solution (a) and exact solution (b).

solution on Γ_r. Compared with two figures, we can conclude that the projection method with regularization is accurate and effective.

6. Conclusion

In this paper, we propose a projection method with regularization for solving the Cauchy problem for the Helmholtz equation in the exterior of a bounded two- or three-dimensional case. This problem is transformed into a compact operator equation. The asymptotic behaviors of singular values for the compact operator are analyzed, and the convergence for the numerical algorithm is discussed. The numerical examples demonstrate that our method is consistent, effective and less sensitive to the random noises.

References

[1] D.E. Beskos, Boundary element methods in dynamic analysis: Part II (1986-1996), *ASME Appl. Mech. Rev.*, **50**:3 (1997), 149–197.

[2] D. Colton and R. Kress, Integral Equation Methods in Scattering Theory, Wiley, New York, 1983.

[3] D. Colton and R. Kress, Inverse Acoustic and Electromagnetic Scattering Theory, 2nd edition, Springer-Verlag, New York, 1998.

[4] J.T. Chen, Recent development of dual BEM in acoustic problems, *Comput. Method Appl. M.*, **188**:4 (2000), 833–845.

[5] Z.M. Chen and X.Z. Liu, An adaptive perfectly matched layer technique for time-harmonic scattering problem, *SIAM J. Numer. Anal.*, **43** (2005), 645–671.

[6] T. Delillo, V. Isakov, N. Valdivia and L. Wang, The detection of the source of acoustical noise in two dimensions, *SIAM J. Appl. Math*, **61** (2001), 2104–2121.

[7] T. Delillo, V. Isakov, N. Valdivia and L. Wang, The detection of surface vibrations from interior acoustical pressure, *Inverse Probl.*, **19** (2003), 507–524.

[8] L. Eldén , F. Berntsson and T. Regińska, Wavelets and Fourier methods for solving the sideways heat equation, *SIAM J. Sci. Comput.*, **21** (2000), 2187–2205.

[9] F. Natterer, Aninitial value approach to the inverse Helmholtz equation problem at fixed frequency, *Inverse Problems in Medical Imaging and Nondestructive (Oberwolfach, 1996)*, Springer, Vienna, (1997), 159–167.

[10] I. Harari, P.E. Barbone, M. Slavutin and R. Shalom, Boundary infinite elements for the Helmholtz equation in exterior domains, *Int. J. Numer. Meth. Eng.*, **41** (1998), 1105–1131.

[11] P.C. Hansen, The L-curve and its use in the numerical treatment of inverse problems, *In: Johnston (Ed.), Computational Inverse Problems in Electrocardiology, WIT Press, Southampton*, (2001), 119–142.

[12] I. Harari, A survey of finite element methods for time-harmonic acoustics, *Comput. Method. Appl. M.*, **195** (2006), 1594–1607.

[13] V. Isakov, Inverse Problems for Partial Differential Equations, Springer-Verlag, New York, 1998.

[14] V. Isakov and S.F. Wu, On theory and application of Helmholtz equation least squares method in inverse acoustic problems, *Inverse Probl.*, **18** (2002), 1147–1159.

[15] B.T. Jin and Y. Zheng, Boundary knot method for some inverse problems associated with the Helmholtz equation, *Int. J. Numer. Meth. Eng.*, **62** (2005) 1636–1651.

[16] B.T. Jin and L. Marin , The plane wave method for inverse problems associated with Helmholtz-type equations, *Eng. Anal. Bound. Elem.*, **32** (2008) 223–240.

[17] V.A. Kozlov and V.G. Maźya, On iterative procedures for solving ill-posed boundary value problems that preserve differential equations, *Lenningr. Math. J.*, **1**:5 (1990), 1207–1228.

[18] V.A. Kozlov, V.G. Maźya and A.V. Fomin, An iterative method for solving the Cauchy problem for elliptic equations, *Comput. Maths. Math. Phys.*, **31** (1992), 45–52.

[19] A. Kirsch, An Introduction to the Mathematical Theory of Inverse Problem, Springer-Verlag, NewYork, 1996.

[20] W. McLean, Strongly Elliptic Systems and Boundary Integral Equations, Cambridge University Press, Cambridge, 2000.

[21] L. Marin, L. Elliott, P.J. Hegges, D.B. Ingham, D. Lesnic and X.Wen, An alternating iterative algorithm for Cauchy problem associated to the Helmholtz equation, *Comput. Method. Appl. M.*, **192** (2003), 709–722.

[22] L. Marin, L. Elliott, P.J. Hegges, D.B. Ingham, D. Lesnic and X.Wen, Conjuate gradient boundary element solution to the Cauchy problem for Helmholtz-type equations, *Comput. Mech.*, **31** (2003), 367–377.

[23] L. Marin and D. Lesnic, The method of fundamental solutions for Cauchy problem associated with two-dimensional Helmholtz-type equations, *Comput. Struct.*, **83** (2005), 267–278.

[24] L. Marin, Boundary element-minimal error method for the Cauchy problem associated with two-dimensional Helmholtz-type equations, *Comput. Mech.*, **44** (2009), 205–219.

[25] M. Reed and B. Simon, Methods of Mordern Mathematical Physics IV : Analysis of Operators, Academic Press, 1978.

[26] T. Regińska and K. Regiński, Approximate solution of a Cauchy problem for the Helmholtz equation, *Inverse Probl.*, **22**(2006), 975–989.

[27] X.T. Xiong and C.L. Fu, Two approximate methods of a Cauchy problem for the Helmholtz equation, *Comput. Appl. Math.*, **26** (2007), 285–307.

[28] T. Wei, H.H. Qin and R. Shi, Numerical solution of an inverse 2D Cauchy problem connected with the Helmholtz equation, *Inverse Probl.*, **24** (2008), 1–18.

[29] H.H. Qin, T. Wei and R. Shi, Modified Tikhonov regularization method for the Cauchy problem of the Helmholtz equation, *J. Comput. Appl. Math.*, **224** (2009), 39–53.

[30] C. Yu, Z.F. Zhou and M. Zhuang, An acoustic intensity-based method for reconstruction of radiated fields, *J. Acoust. Soc. Am.*, **123** (2008), 1892–1901.

[31] C. Yu, Z.F. Zhou , M. Zhuang, X.D. Li and F. Thiele, 3-D acoustic intensity-based method and its CAA applications, *14th AIAA/CEAS Aeroacoustic Conference (29th Aeroacoustic Conference), 5-7 May, Vancoucer British Columbia Canada*, 2008.